Optical Properties and Piezoreflectance of Silver-Palladium Alloys*

B. F. Schmidt† and D. W. Lynch
Institute for Atomic Research and Department of Physics, Iowa State University, Ames, Iowa 50010
(Received 8 April 1970; revised manuscript received 18 December 1970)

Normal-incidence reflectance and transmittance measurements were made on thin vacuum-evaporated films of five silver-palladium alloys, approximately 1000 Å thick, containing from 0 to 15 at.% palladium. In addition, the fractional change in reflectance with strain was measured for films of four Ag-Pd alloys having Pd concentrations from 0 to 4 at.%. The data yielded the dielectric constant $\tilde{\epsilon}$ and the change in the dielectric constant with strain from 1.8 to 4.6 eV. The peak in the loss function, $-\mathrm{Im}(1/\tilde{\epsilon})$, near 3.8 eV decreases and broadens rapidly with alloying. An overlap between the loss-function peak and an absorption band due to transitions from resonant bound states on the Pd sites indicates that excitation of quasilocalized electrons is an important mechanism for the damping of plasma oscillations in the alloys. The 3.87-eV absorption edge in pure silver broadens with alloying, but does not shift noticeably. With the aid of the piezoreflectance data, the energy of the two transitions, $L_3 \rightarrow$ (Fermi surface) and $L_{2'} \rightarrow L_1$, contributing to this edge have been located. The former begins at approximately 3.88 eV for silver and the edge for the latter, corresponding to the energy difference between the Fermi energy and a state in the second conduction band passing through L_1, occurs at 3.98 eV. The energy difference between L_1 and L_2 was determined to be 4.25 eV in silver. Errors in the Kramers-Kronig transform of the piezoreflectance spectrum are shown to introduce fine structure in the spectrum of the strain derivative of the dielectric constant.

INTRODUCTION

A study of the optical properties of silver and silver-based alloys yields information on the band structure of silver and how the bands are altered by solutes, on the charge carriers in silver, and on collective effects in silver and its alloys. Two preceding papers (to be called ML1 and ML2) dealt with dilute alloys of indium in silver.[1,2] In the following we discuss measurements of the optical constants and piezoreflectance of alloys of silver with up to 15 at.% palladium.

The first interband absorption edge in silver seems[3-5] to be caused by strong transitions from the uppermost d band to the Fermi surface near L (i.e., transitions near $L_3 \rightarrow L_{2'}$), overlapped by weaker transitions from the neck of the Fermi surface near L, and states just below it, to a higher conduction band (i.e., transitions near and including $L_{2'} \rightarrow L_1$). Adding indium to silver causes the former transitions to shift to higher energy and the latter to lower energy. The two overlapping transitions can be distinguished by photoemission[5] and by piezoreflectance[2] measurements. Piezoreflectance measurements allow one to detect the weaker interband transitions ($L_{2'} \rightarrow L_1$) in this case because they are more strain sensitive than the stronger $L_3 \rightarrow L_{2'}$ transitions.

The addition of palladium, instead of indium, to silver might be expected to cause the transitions to shift in directions opposite to those found upon addition of indium, but that is not what happens. Extensive work on the addition of transition-metal solutes to noble metals has been carried out recently.[6-12] It shows[6-11] that the 10 Pd $4d$ levels overlap the filled s-p conduction band. This overlap causes a localized quasibound resonant state to form, a state which is occupied by about 9.6 electrons per Pd atom.[11] This state gives a peak in the density of states about half-way between the Fermi level and the top of the d band. The resonant state slightly overlaps both the d band and Fermi level. The potential of the bare Pd^+ ion is partially screened by the "extra" localized electronic charge ($\sim 0.6e$)[11] so that it resembles the potential of a silver ion. The interband absorption edge then is not noticeably shifted. The excitation of quasibound electrons at Pd sites has been observed,[6-8,12] and is a prominent part of the spectrum between 1 and 4 eV for palladium concentrations above 5%.

In the following, we confirm the negligible effect of Pd on the interband edge in silver.[7] We also

TABLE I. Palladium concentrations (at.%).

Bulk starting material	Films for R and T	Films for piezoreflectance
1.8	•••	1.2±0.2
5.8	2.4±0.3	2.3±0.3
8.5	4.2±0.5	4.1±0.5
16.2	7.0±1.0	•••
26.3	14.8±3.0	•••

show the effect of Pd on the plasmons in silver. It is seen that in alloys containing 10% Pd, at least 25% of the plasmon damping arises from the excitation of electrons localized about Pd sites. "New" sources of error in piezoreflectance measurements are discussed. We report a revised value of 4.25 eV for the $L_{2'} \rightarrow L_1$ band gap in pure silver, this value being derived from piezoreflectance measurements in which both $L_3 \rightarrow L_{2'}$ and $L_{2'} \rightarrow L_1$ transitions provide structure.

EXPERIMENTAL

Sample Preparation

All measurements were made on evaporated films on substrates of fused quartz or polished lead zirconate-lead titanate piezoelectric transducers. The films were evaporated in a vacuum of 2×10^{-7} Torr or less. Because of the great disparity in constituent vapor pressures, flash evaporation was used. For each set of films, about 100 small pieces of a bulk alloy sample were dropped onto a hot filament, one evaporating before the next was dropped. The films were then annealed in the evaporator at 310 °C for 24 h. Film compositions were determined by x-ray diffraction measurement of the lattice parameters.[13] As the Pd concentration increased, the Debye-Scherrer rings broadened, increasing the uncertainty in lattice parameter, hence in composition. (Without annealing, no diffraction rings could be seen.) All films were Pd deficient with respect to the bulk alloy from which they were prepared (Table I).

The films on quartz were semitransparent, and ranged from 800 to 1200 Å in thickness. Film thickness was measured by multiple-beam interferometry. Films of several thicknesses were produced in each evaporation, and no thickness dependence of the optical properties was found. The films on the transducers were about 10 000 Å thick, thick enough to be considered opaque.

Optical Constants

The reflectance R and transmittance T of the films on quartz were measured at room temperature between 1.8 and 5.4 eV on a Cary 14R spectrophotometer. The spectral bandpass was about 0.02 eV. A reflectometer like that of Hartman and Logothetis[14] was used. The reflectance measurements were made with the light incident through the quartz to reduce the effect on the reflectance measurement of the oxidation of the outer surface of the film. The real and imaginary parts of the refractive index n and k were found from the measured values of R and T by an iterative method on a computer. Several iterations provided a numerical accuracy of 0.001. Above about 4 eV this method is very poor for silver.[1] Small uncertainties in R and T lead to a very large uncertainty in n. Moreover, annealing the films, a necessity for homogeneity of the alloys, causes the films to have anomalously low reflectivities.[15] Above 3 eV, the reflectivity was replaced by ϕ, the phase shift of the transmitted amplitude. T is less affected by annealing than R, and small errors in ϕ do not cause large errors in n. ϕ was obtained from a Kramers-Kronig analysis of T, while n and k were obtained from T and ϕ by an iteration scheme.[15] We display our results to 4.6 eV although ϕ was computed to 5.4 eV, using T data to 5.4 eV and an extrapolation for higher photon energy.

From n and k, the real and imaginary parts of the complex dielectric constant ϵ_1 and ϵ_2 can be obtained:

$$\epsilon_1 = n^2 - k^2 , \tag{1}$$

$$\epsilon_2 = 2nk . \tag{2}$$

Piezoreflectance

The method developed by Engler *et al.*[16,17] was used. The ceramic transducers were driven at 1.1 kHz by 940 V peak to peak, causing a uniform planar expansion and contraction of the face on which the film was deposited. The peak linear strain in one direction in the face, $\Delta l/l$, was estimated to be 4.1×10^{-5}. Spectra of $\Delta R/R$, the strain-induced relative change of the reflectance, were recorded from 1.8 to 4.6 eV, using the apparatus of ML2.

The baseline on these recordings is shifted spuriously by motion of the inhomogeneous light beam across the photocathode, synchronous with the piezoreflectance signal.[17] The baseline was adjusted so that for each alloy, at 1.80 eV, the value of $\Delta R/R$ was that expected for a free-electron gas. This shift was assumed to be wavelength independent. The reflectivity at normal incidence is

$$R = \frac{(n-1)^2 + k^2}{(n+1)^2 + k^2} . \tag{3}$$

For a free-electron gas,

$$\epsilon_1^f = 1 - \frac{\omega_p^2 \tau^2}{1+\omega^2\tau^2} , \tag{4}$$

$$\epsilon_2^f = \frac{\omega_p^2 \tau}{\omega(1+\omega^2\tau^2)} , \tag{5}$$

where τ is a relaxation time and ω_p is the plasma frequency,

$$\omega_p^2 = 4\pi N e^2/m^* , \tag{6}$$

with N, the carrier concentration and m^*, the effective mass. From Eqs. (1)–(6), $\Delta R/R$ for a free-electron gas can be found if values for ω_p, τ, and their strain derivatives can be found. The strain derivatives are

$$\frac{\Delta\omega_p}{\omega_p} = -\frac{1}{2}\frac{\Delta V}{V}, \tag{7}$$

$$\frac{\Delta\tau}{\tau} = \frac{\Delta V}{V} - \frac{\Delta\rho}{\rho} = \left[1 - \frac{\partial \ln\rho}{\partial \ln V}\right]\frac{\Delta V}{V}, \tag{8}$$

if m^* is not altered by strain and if the low-frequency value of τ can be used. V is the film volume and ρ is its resistivity. (Shear strain should have no effect on a free-electron gas.) Now $\Delta V/V \approx \Delta l/l$ since the thickness of the film decreases by about the same fraction as one side expands, and $\Delta\rho/\rho$ can be obtained from data on the resistivity of Ag-Pd alloys as a function of strain.[18] We used $\hbar\omega_p = 9.20$ eV for pure silver, and assumed ω_p was proportional to the square root of the silver concentration in the alloys. This has some theoretical justification,[9] and such a dependence was observed by Myers *et al.*,[7] although their value for ω_p for pure silver may be in error, due to the small film thicknesses necessary for their infrared transmission measurements. τ for pure silver was obtained from Eq. (5) at 1.8 eV where there are no other contributions to the complex dielectric constant. Matthiessen's rule was assumed to hold for the alloys at optical frequencies:

$$\tau^{-1} = \tau_0^{-1} + \tau_c^{-1}, \tag{9}$$

where τ is the relaxation time of the alloy film, τ_0 that of the pure silver film, and τ_c^{-1} the increase in scattering rate due to the solute. The low-frequency value of τ_c^{-1} increases linearly with Pd concentration[19] and the same increase was used for our data. The resultant free-electron parameters are given in Table II. The baseline corrections to the $\Delta R/R$ spectra were from 2 to 20% of the peak height of the structure above the original baseline. A possible error in this subtraction procedure arises from the neglect of the low-frequency contribution of interband transitions to ϵ_1. Equation (4) should then have a constant ϵ_1^b added to it, and this constant can vary with volume strain and shear strain. This will be discussed later.

TABLE II. Free-electron gas parameters.

Alloy (at.% Pd)	$\hbar\omega_p$ (eV)	τ (10^{-15} sec)	$\frac{\partial \ln\rho}{\partial \ln V}$
0.0	9.20	10.4	4.7
1.2	9.15	9.4	4.3
2.3	9.10	8.8	3.9
2.4	9.09	8.7	•••
4.1	9.01	8.1	3.4
4.2	9.00	8.0	•••
7.0	8.88	7.4	•••
14.8	8.50	6.3	•••

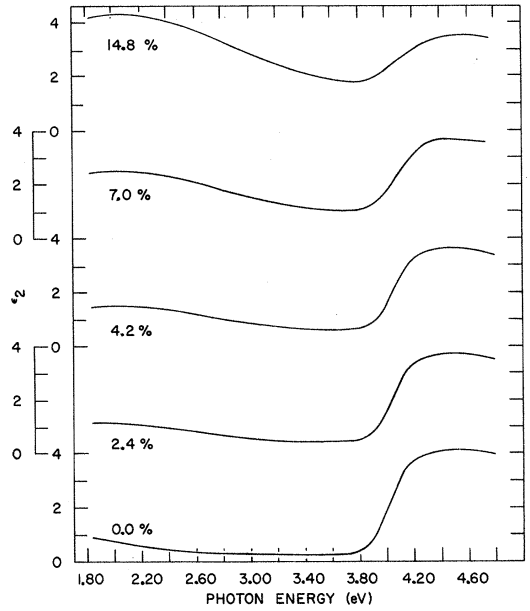

FIG. 1. Imaginary part of the complex dielectric constant ϵ_2 vs photon energy for Ag and Ag-Pd alloys.

RESULTS

The spectra of the imaginary part of the complex dielectric constant are shown in Fig. 1. The data (and those for ϵ_1) for pure silver agree well with those of ML1 and others.[20] The dielectric constant data have the same shape as those of Ref. 7, but we feel our accuracy is sufficiently high to let us

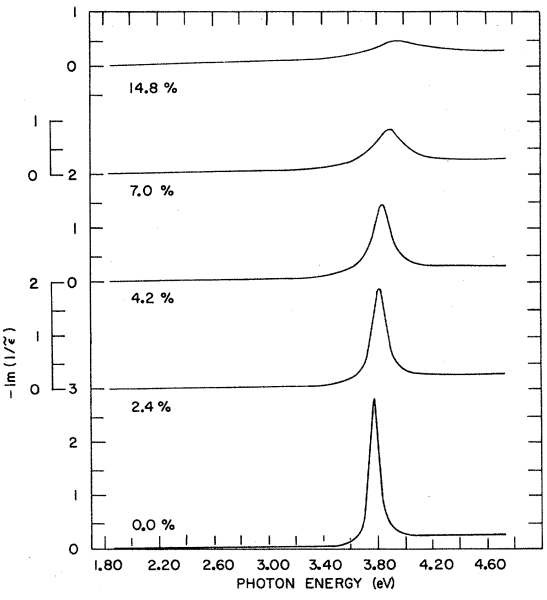

FIG. 2. Loss function, $-\mathrm{Im}(\tilde{\epsilon}^{-1})$, vs photon energy for Ag and Ag-Pd alloys.

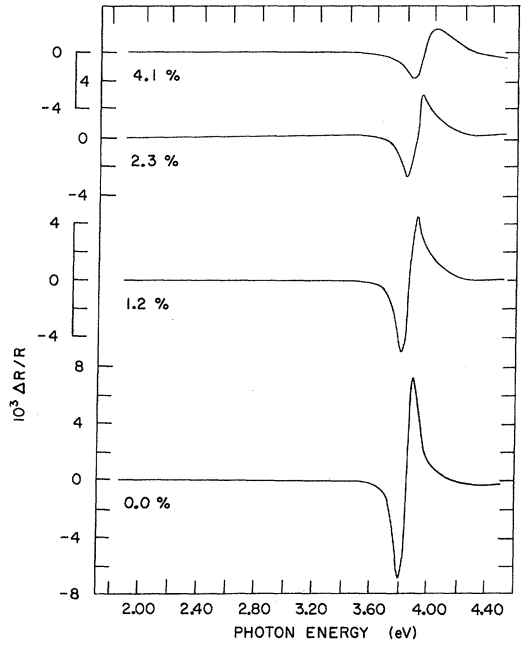

FIG. 3. The strain-induced relative change in reflectivity $\Delta R/R$ vs photon energy for Ag and Ag-Pd alloys. Pd concentration in at.%. The strain was a combination of shear strain and hydrostatic strain applied to polycrystalline partly oriented samples.

calculate plasmon effects with our data. (For a discussion of errors, see the Appendix.) The imaginary part of the inverse dielectric constant is shown in Fig. 2. It is

$$\mathrm{Im}(\tilde{\epsilon}^{-1}) = \epsilon_2/(\epsilon_1^2+\epsilon_2^2)\,, \tag{10}$$

and is proportional to the probability that a fast electron will lose energy E, the argument of $\tilde{\epsilon}$, by producing excitations in the volume of the system.[21,22]

$\Delta R/R$ is shown in Fig. 3. From this $\Delta\theta$, the strain-induced change of the phase shift of the reflected amplitude, can be obtained by Kramers-Kronig analysis.[2,17] Then the strain-induced changes in the dielectric constant components are

$$\Delta\epsilon_1 = \tfrac{1}{2}[n(\epsilon_1-1)-k\epsilon_2](\Delta R/R)+[k(\epsilon_1-1)+n\epsilon_2]\Delta\theta$$

$$= \tfrac{1}{2}A(\Delta R/R)+B\,\Delta\theta\,, \tag{11}$$

$$\Delta\epsilon_2 = \tfrac{1}{2}[k(\epsilon_1-1)+n\epsilon_2](\Delta R/R)-[n(\epsilon_1-1)-k\epsilon_2]\Delta\theta$$

$$= \tfrac{1}{2}B(\Delta R/R)-A\,\Delta\theta\,. \tag{12}$$

Unfortunately it was not possible to use identical samples for measurements of both $\Delta R/R$ and R, T. The values of n, k, ϵ_1, and ϵ_2 used in (11) and (12) were obtained at each energy from those of the R, T samples by a least-squares interpolation, quadratic in the Pd concentration. The resultant $\Delta\epsilon_2$ spectra are shown in Fig. 4.

DISCUSSION

ϵ_2 and Im $(\tilde{\epsilon}^{-1})$

From Fig. 1 it is clear that the addition of palladium to silver does not significantly shift the first interband absorption edge. This was reported and interpreted by Myers *et al.*[6,7] and is quite different from the effects of the addition of Zn, Cd,[23] and In[1] on the edge. There is additional broadening as Pd is added, but again the effect is small when compared with that of In addition. The dielectric constant can be written as the sum of two terms, $\tilde{\epsilon}^f$ due to the free-electron gas [(Eqs. (4) and (5)] and $\tilde{\epsilon}^b$ due to interband transitions. ϵ_2^b is of interest for comparison with band structures, and was found by subtracting ϵ_2^f from the measured ϵ_2, using the parameters in Table II to evaluate ϵ_2^f. Plots of ϵ_2^b or $\omega\epsilon_2^b$ (the transition probability) vs $\hbar\omega$ each have a reasonably straight section on the absorption edge. When extrapolated to zero ϵ_2^b or $\omega\epsilon_2^b$ these give an energy of 3.87 eV for the "onset" of the first interband absorption in silver and the two most dilute alloys. The two more concentrated alloys have intercepts at slightly lower energies, but this is not very meaningful because of overlap of the edge with the broad peak rising near 2.6 eV.

The broad peak near 2.6 eV has been studied and interpreted by Myers *et al.*[6,7] in Ag-Pd as well as in other similar systems. It appears to be a transition from a virtual bound state on the Pd site be-

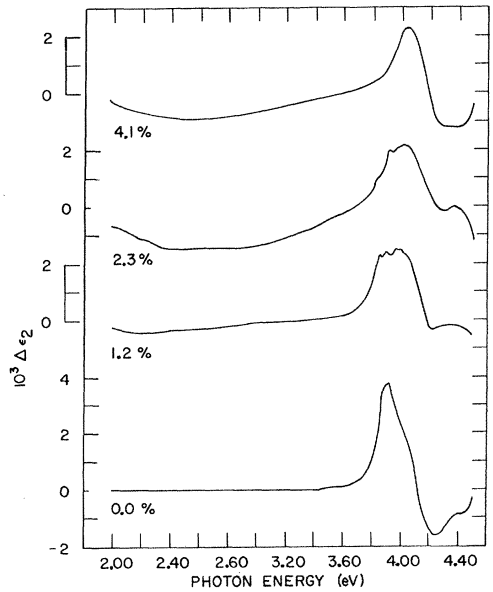

FIG. 4. The strain-induced change in the imaginary part of the refractive index $\Delta\epsilon_2$ vs photon energy for Ag and Ag-Pd alloys.

low the Fermi level, but above the Ag d band, to states at and above the Fermi level. Most, but not all (1.4 eV of 1.8 eV), of the width of the absorption peak arises from the width of the initial state, as judged by photoemitted electrons originating from this state.[8] Kjöllerström[10] has discussed the shape and oscillator strength of this peak. The tail of this peak overlaps the absorption edge to a considerable extent in our two more concentrated alloys. By extrapolating the 2.6-eV peak, one finds that roughly 25–50% of ϵ_2^b at 3.9 eV arises from the localized states in the 7%-Pd alloy. The curves of Fig. 2 show that plasmons are well-defined excitations in Ag-Pd for Pd concentrations up to around 5%. At higher concentrations, they damp rapidly and by 15% Pd they are not well-defined entities. This damping is due to the increase in ϵ_2 near $\omega \approx \omega_p$.[24,25] For Ag and the more dilute Ag-Pd alloys, free-carrier damping and interband damping predominate, i.e., the plasmons decay by exciting intraband or interband transitions. By 7% Pd, an appreciable fraction of ϵ_2 arises from transitions of the quasibound electrons at the Pd sites. This fraction reaches at least 25% by 10% Pd. This is a new source of plasmon damping. A proper microscopic calculation of the dielectric constant[26] for this system should include the virtual bound states, and should show a coupling between modes which are predominantly plasmonlike and prodominantly virtual bound states, as well as coupling between plasmons and one-electron interband excitations. (Kjöllerström's calculation of $\tilde{\epsilon}^f$ does include free-electron damping by excitation of virtual bound states.[10])

$\Delta\epsilon_2$ Spectra

As emphasized in ML2, the spectra of $\Delta\epsilon_2$ are more reliably interpreted than those of $\Delta R/R$. $\Delta\epsilon_2^b$ is of more interest than $\Delta\epsilon_2$, but estimates of $\Delta\epsilon_2^f$ show that it is very small near the interband edge, less than 0.04×10^{-3} at 3.6 eV, so that for our purposes $\Delta\epsilon_2 = \Delta\epsilon_2^b$.

There are three types of structure in $\Delta\epsilon_2$ (Fig. 4): (i) All samples show a large peak near 3.9–4.0 eV, followed by a negative peak near 4.2 eV. Silver shows a shoulder at 4.0 eV as well. (ii) Two of the alloy samples have "fine structure" between 3.8 and 4.0 eV, on the main peak. (iii) All alloys have a rise in $\Delta\epsilon_2$ below about 2.40 eV and a broad region of negative $\Delta\epsilon_2$ between 2.4 and 3.6 eV. (We disregard the rapid "takeoff" of $\Delta\epsilon_2$ at the high-energy limit of the data. Errors in $\Delta\theta$ because of the limited $\Delta R/R$ range and the extrapolation of $\Delta R/R$ become very large here.) These structures are partly the result of structure in $\Delta R/R$ (hence $\Delta\theta$) and partly due to the functions of n and k, A and B of Eqs. (11) and (12), which multiply them. Thus our curve for $\Delta\epsilon_2$ for pure silver differs somewhat from that displayed in previous measurements, although the $\Delta R/R$ curves agree well. Engeler *et al.*[17] used literature values of n and k for bulk silver,[27,28] while ML2 and we used data obtained on films. (ML used the data of Ref. 1. We remeasured n and k of silver.) In ML2 one finds curves of A and B [Eqs. (11) and (12)] which are smooth functions of photon energy, implying that structure in $\Delta\epsilon_2$ arises primarily from structure in $\Delta R/R$ and $\Delta\theta$. Figure 5 shows the individual contributions to $\Delta\epsilon_2$, $\frac{1}{2}A\,\Delta R/R$, and $-B\Delta\theta$. It is clear there that both curves have considerable structure which tends to cancel upon addition. Small errors in n and k can lead to incomplete cancellation in the free-electron region, and to altered structure in the interband region. Errors in either the shape or over-all magnitude of the $\Delta\theta$ spectrum from extrapolation in the Kramers-Kronig integrals lead to similar errors.

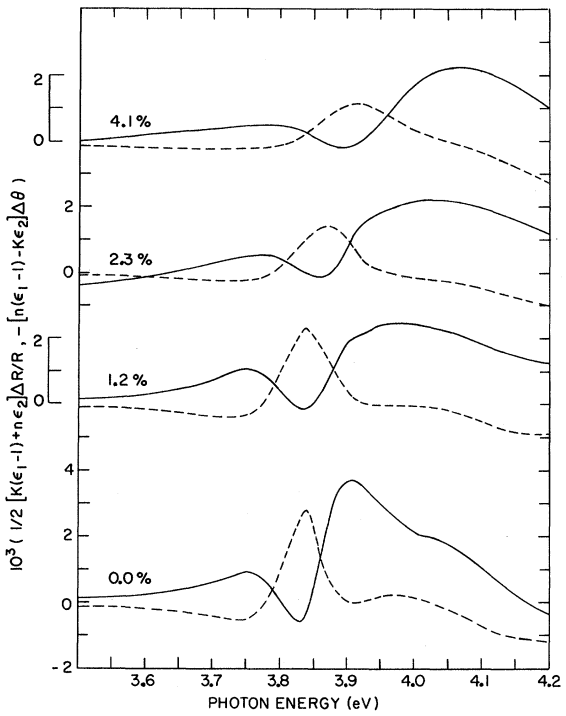

FIG. 5. The individual contributions to $\Delta\epsilon_2$ from $\Delta R/R$ (solid lines) and from $\Delta\theta$ (dashed lines) vs photon energy for Ag and Ag-Pd alloys. The sum of the two curves for each alloy is the corresponding curve in Fig. 4.

We have attempted to study the effect of errors on the three types of structure mentioned previously. We first assumed a constant 5% error in n (see the Appendix) and recomputed $\Delta\epsilon_2$ for Ag and Ag + 1.2% Pd. In both cases the large peak in $\Delta\epsilon_2$ was increased in height by about 10% and sharpened because the wings decreased. The "fine structure"

in the alloy $\Delta\epsilon_2$ spectrum was not altered. The region of negative $\Delta\epsilon_2$ below 3.6 eV and the low-energy rise of $\Delta\epsilon_2$ in the alloy were shifted slightly, but did not tend to disappear. All features of $\Delta\epsilon_2$ vs E are thus *qualitatively* insensitive to errors in A and B arising from errors in the optical constants.

$\Delta\theta$ can have much larger errors than n (see Appendix). We recomputed $\Delta\epsilon_2$ using the measured $\Delta R/R$ and the $\Delta\theta$ computed by Kramers-Kronig analysis, but with $\Delta\theta$ multiplied by 0.75 or 1.25. The results are shown in Figs. 6 and 7. It is clear that in Ag, the major structures, the peak at 3.9 eV, and the shoulder at 4.0 eV are not significantly altered by such a large, but possible, error in $\Delta\theta$. For the 1.2% alloy, the main peak at 4.0 eV and the long tail from 3.6 to 3.9 eV also are not seriously affected, but some of the fine structure is enhanced when $\Delta\theta$ is multiplied by 1.25 and diminished when 0.75 $\Delta\theta$ is used. Figure 7 also shows that this fine structure occurs at some, but not all, of the peaks in $\Delta R/R$ or $\Delta\theta$. The largest one, at 3.85 eV is probably a result of an error in the $\Delta\theta$ peak, which could be produced directly by errors in the $\Delta R/R$ peaks at 3.80 and 3.90 eV or by a general level shift of the $\Delta\theta$ curve due to the extrapolation in the Kramers-Kronig integral. It thus appears that the fine structure in $\Delta\epsilon_2$ for the two dilute alloys is an artifact of the Kramers-Kronig integration, and should be disregarded. The assumed errors in $\Delta\theta$ have little effect on $\Delta\epsilon_2$ between 1.8 and 3.4 eV. The rise in $\Delta\epsilon_2$ at low energy for the alloys is a genuine effect and represents the free-carrier contribution to $\Delta\epsilon_2$, but it has large errors in it because the functions A and B become very large at low energy. The rise is not seen in pure silver because $\Delta\epsilon_2^f$ is expected to

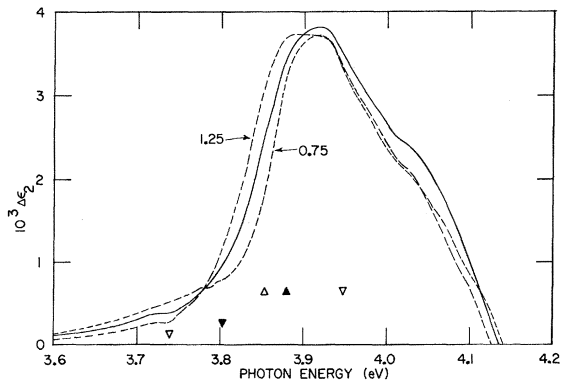

FIG. 6. $\Delta\epsilon_2$ for pure silver, solid line, as in Fig. 4; dashed lines, using 1.25 $\Delta\theta$ and 0.75 $\Delta\theta$ instead of $\Delta\theta$ in Eqs. (11), (12). The solid triangles pointing up (down) indicate the positions of positive (negative) peaks in $\Delta R/R$. The open triangles give the same for $\Delta\theta$.

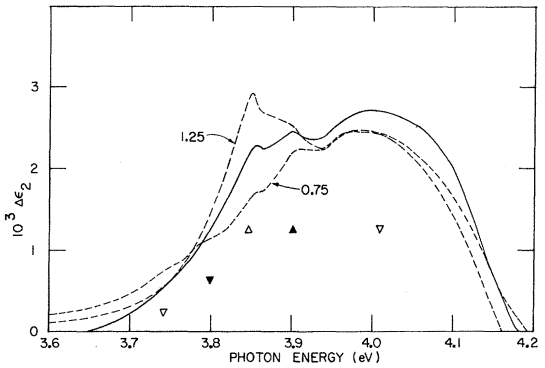

FIG. 7. $\Delta\epsilon_2$ for Ag+1.2% Pd. The key is the same as for Fig. 6.

be smaller there. The negative structureless region in $\Delta\epsilon_2$ between about 2 and 3.4 eV for the alloys is believed to be an artifact of the baseline subtraction. It seems not to be the result of neglecting $\Delta\epsilon_1^b$, the strain dependence of ϵ_1^b at low energy, for we have obtained values of $\Delta\epsilon_1^b$ at low energies which are too small to affect the baseline shift very much.

$\Delta\epsilon_2$ for pure silver begins around 3.8 eV, peaks at 3.92 eV, with a shoulder on this peak at about 4.0 eV, followed by a negative peak. The 3.92-eV peak has been observed before,[17] while the 4.0-eV shoulder is new. The three alloys all exhibit a peak between 4.00 and 4.04 eV. This peak is the same height in all three alloys and has the same position and height as the shoulder at 4.0 eV in silver. The peak at 3.92 eV in silver does not appear as a peak in any of the alloys, but there is a large low-energy tail of the 4.00–4.04-eV peak. In the 1.2% alloy, there may be a shoulder at 3.85 eV (Fig. 7) but not a peak. Hence the 3.92-eV peak in silver disappears upon alloying with Pd, possibly becoming a broad tail on the low-energy side of the 4.0-eV peak.

None of the alloys show any structure between 2 and 3 eV that cannot be ascribed to errors in baseline correction or Kramers-Kronig analysis. The lack of a piezoreflectance signal from the transitions of quasibound electrons is understandable, because they produce broad structure in ϵ_2 and because the states are localized around Pd sites, hence are expected to be strain insensitive. [The expected $\Delta\epsilon_2$ signal[2] should be proportional to $-(d\epsilon_2/dE)(dE_{ij}/de)e$, where E_{ij} is the energy difference between the initial and final states of the transition, and e is the applied strain.] Moreover, no additional structure was found in $\Delta R/R$ between 3.0 eV and the large negative peak at 3.80 eV in pure silver. Such structure was reported by Engeler *et al.*[17] and tentatively assigned to surface plasmons on rough surfaces[29–31] by ML2. The origin

of the original structure in $\Delta R/R$ is not clear, but that structure in $\Delta R/R$ due to surface plasmons should be very small now seems likely. Jasperson and Schnatterly[30] show that instead of having a resonancelike shape (as stated in ML2), the surface-plasmon absorption in silver produces a broad reduction in the reflectivity beginning at fairly low energy and ending near 3.6 eV, where $\epsilon_1 = -1$. Reflectivity measurements made on our piezoreflectance samples of Ag indicated a broad "loss" of reflectivity when compared with the reflectivity of Ag films on smoother quartz substrates. Such broad structure is difficult to detect in a modulation experiment.

It is reasonable that the 3.92-eV peak is the result of the $L_3 \rightarrow L_{2'}$ transition. This transition gives rise to the absorption edge in silver, the $L_{2'} \rightarrow L_1$ transitions in silver occurring at somewhat higher energy. The 4.0-eV shoulder probably arises from the $L_{2'} \rightarrow L_1$ transitions. If these assignments were interchanged, one would expect to see structure on the edge in ϵ_2, as occurs in Ag-In alloys, because then the lower-energy transition would be the weaker of the two. The 3.92-eV peak occurs within 0.05 eV of the absorption edge as previously "defined," and within 0.05 eV by any other reasonable criterion.

The shape of the $\Delta\epsilon_2^b$ signal expected from the $L_{2'} \rightarrow L_1$ transition was discussed in ML2. This shape is proportional to $d\epsilon_2/dE$ for the transitions near $L_{2'} \rightarrow L_1$. $L_{2'} \rightarrow L_1$ transitions have a critical point in the joint density of states of type M_2, while at slightly lower energy, the transitions begin rather sharply as the Fermi statistics suddenly allow the transition to occur.[32,33] Then, neglecting broadening, the $\Delta\epsilon_2^b$ spectrum consists of a positive (or negative) peak at the energy difference between the Fermi surface and the upper band, followed by a negative (positive) peak at the energy difference between the bands at $L_{2'}$ and L_1. The sign uncertainty is due to the sign of the difference in deformation potentials of the bands, the former signs fitting experiment. The transitions near $L_3 \rightarrow L_{2'}$ begin suddenly as the Fermi statistics allow them to occur, then persist for several electron volts without sharp structure in ϵ_2. The $\Delta\epsilon_2^b$ spectrum then should consist of one positive (negative) peak at the onset of transitions, i.e., at the energy difference between the Fermi level and the d band near L_3. Any further $\Delta\epsilon_2^b$ structure from this transition near 4 eV should be small because the joint density of states has no sharp structure except for its initial rise near 3.9 eV. The positive sign agrees with our data (see Fig. 8). In silver we identify the peak in $\Delta\epsilon_2$ at 3.92 eV with $L_3 \rightarrow L_{2'}$ transitions, the shoulder at 4.0 eV as the positive peak from the $L_{2'} \rightarrow L_1$ transitions, and the negative peak at higher energy with the $L_{2'} \rightarrow L_1$ transitions.

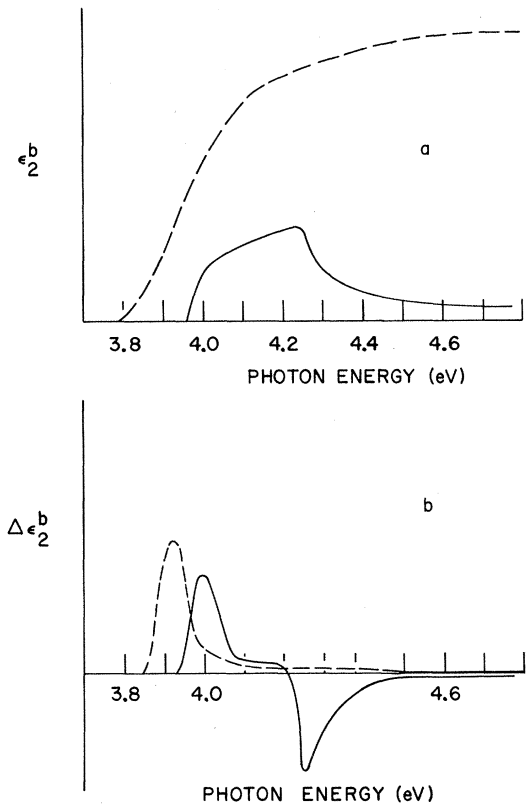

FIG. 8. Schematic decompositions of ϵ_2^b and $\Delta\epsilon_2^b$ for silver into its contributions from transitions near $L_{2'} \rightarrow L_1$ (solid) and $L_3 \rightarrow L_{2'}$ (dashed).

On the basis of the shape analysis of the $\Delta\epsilon_2^b$ described in ML2, we assign to the energy gap $L_1 \rightarrow L_{2'}$ the value 4.25 eV, and the gap from the Fermi surface to the band directly above it (near L_1) is 3.98 eV in pure Ag. The uncertainty in these values is about 0.03–0.05 eV.

By superimposing the $\Delta\epsilon_2$ spectra of all samples, we see that the peaks in $\Delta\epsilon_2$ for the alloys lie at the same energy as the 4.0-eV shoulder in silver, and both alloys and silver have a negative peak at higher energies, although this is distorted by errors in $\Delta\theta$. Thus the $L_{2'} - L_1$ structure persists in the alloys, and is shifted less than 0.05 eV, despite the sensitivity of the L_1 level to crystal potential. The small shift is probably the result of screening of the Pd^+ potential by the quasibound states. The 3.92-eV peak in Ag is replaced by a broad region of positive $\Delta\epsilon_2$ in the alloys, devoid of a peak. The relatively rapid loss, upon alloying with Pd, of the $L_3 \rightarrow L_{2'}$ structure compared to $L_{2'} \rightarrow L_1$ structure is noteworthy. The pure silver films have a preferred orientation: The crystallites have $\langle 100 \rangle$ and $\langle 111 \rangle$ axes normal to the surface, as discussed by Engeler *et al.*[17] We found from x-ray diffraction that adding Pd to Ag caused the $\langle 100 \rangle$ crystallite

orientation to become more preferred than the ⟨111⟩. An estimate of the expected $\Delta\epsilon_2$ spectrum for both types of crystallites, due to volume, trigonal, and tetragonal strains, using Gerhardt's data for copper,[32] leads to the conclusion that loss of ⟨111⟩ crystallites would not explain the loss of the 3.92-eV peak as Pd is added. This loss may simply be a broadening effect. As Pd is added, the low-energy absorption peak merges with the absorption edge, and the states at the top of the silver d band should then acquire some mixed character and broaden. This should broaden that part of ϵ_2^b from these transitions alone, thus broadening the dotted ϵ_2^b edge in Fig. 8(a), and reducing the dotted peak in Fig. 8(b). The center of the virtual level is closer to the top of the d band than to the Fermi level[7,8] (2.3 vs 1.5 eV), so the $L_{2'} \rightarrow L_1$ transition (solid lines in Fig. 8) does not broaden so rapidly.

SUMMARY

Our measurements of $\tilde{\epsilon}$ for Ag-Pd alloys agree with those of Myers *et al.*[7] and allow us to calculate the electron-loss function. The electron loss function and ϵ_2, show that a new plasmon decay process occurs in Ag-Pd alloys, the excitation of quasibound d electrons at Pd sites. Piezoreflectance measurements have revealed a shoulder in $\Delta\epsilon_2$ for pure silver not seen previously. Analysis of the shape of the $\Delta\epsilon$ spectra enables us to identify the contributions from $L_3 \rightarrow L_{2'}$ and $L_{2'} \rightarrow L_1$ transitions. Piezoreflectance spectra are difficult to interpret,[2] and should be converted to $\Delta\epsilon_2$ spectra. We have shown that errors in Kramers-Kronig integrals can give rise to spurious structure, generally small, in the $\Delta\epsilon_2$ spectra, but they do not affect qualitatively the grosser features of the interband $\Delta\epsilon_2$ spectra.

APPENDIX

We estimate that the errors in the measurements of R do not exceed 2%, while the errors in T and the film thickness d each should be less than 2%. These errors are expected to be primarily systematic, and probably have the same sign and magnitude for one film at all wavelengths, and perhaps are nearly the same for all films. Numerical calculations using assumed erroneous values of R, T, and d lead to estimates of about $3\frac{1}{2}$% error in k (largely the result of errors in d) and to errors in n (largely from the R measurement) that increase with increasing energy to about 20% at 4.0 eV for pure silver, but which are considerably smaller for the alloys. Kramers-Kronig analyses of transmission data were used to obtain n between 3 and 4.6 eV. Errors in T and in extrapolation methods yield error estimates of about 6% for n and a shift of no more than 0.01 eV in the position of the peak in ϵ_2. The actual errors should be somewhat smaller, for our data on pure Ag films agree well with those of Ref. 20, which were obtained by a different technique on films kept in a vacuum. (The two sets of optical constants differ by less than 0.1 at all energies.)

For our purposes, it is sufficient to assess the effect of these inaccuracies on the loss function and the piezoreflectance spectrum shape. The loss-function peak for silver occurs very close to the zero of ϵ_1 and has a peak height of about $[\epsilon_2(\omega_p)]^{-1}$. The peak height should be accurate to within about 7%. The peak position, 3.78 eV, also is in good agreement with that obtained from characteristic energy-loss measurements on fast electrons.[34] The error expected in the zero of ϵ_1, i.e., in the energy for which $n = k$, can be found using the slopes dn/dE and dk/dE at the plasma energy. For our errors in n and k, it is 0.005 eV, if we assume no error in the slopes. This is a very small error because of the large slopes.

The largest sources of error in the piezoreflectance measurements are the baseline subtraction for $\Delta R/R$ and the extrapolation of $\Delta R/R$ to higher photon energies. Both of these affect the shape *and magnitude* of the $\Delta\theta$ spectrum, hence $\Delta\epsilon_2$. Errors in measuring $\Delta R/R$ itself should not exceed 5%, except for the baseline. We are unable to determine a meaningful estimate of these errors in $\Delta\theta$, but experience with Kramers-Kronig integrals indicates that the shape of the $\Delta\theta$ spectrum should be "about right" but the magnitude of the features could be off by as much as 100%. We believe our errors are less than this, for the $\Delta\epsilon_2$ we obtain below 3.6 eV agrees well with that expected for a free-electron gas, at least for silver. The effect of errors in n and $\Delta\epsilon$ spectra are discussed in the paper.

---

*Work was performed in the Ames Laboratory of the U. S. Atomic Energy Commission, Contribution No. 2715.

†Present address: Department of Physics, Southwest Missouri State College, Springfield, Mo. 65802.

[1]R. M. Morgan and D. W. Lynch, Phys. Rev. 172, 628 (1968).

[2]C. E. Morris and D. W. Lynch, Phys. Rev. 182, 719 (1969).

[3]D. Beaglehole, Proc. Phys. Soc. (London) 87, 461 (1966).

[4]F. M. Mueller and J. C. Phillips, Phys. Rev. 157, 600 (1967).

[5]C. N. Berglund and W. E. Spicer, Phys. Rev. 136, A1044 (1964); also W. F. Krolikowski and W. E. Spicer (unpublished).

[6]Å. Karlsson, H. P. Myers, and L. Walldén, Solid State Commun. 5, 971 (1967).

[7]H. P. Myers, L. Walldén, and Å. Karlsson, Phil.

Mag. 18, 725 (1968).
[8]C. Norris and P. O. Nilsson, Solid State Commun. 6, 649 (1968).
[9]B. Kjöllerström, Solid State Commun. 7, 705 (1969).
[10]B. Kjöllerström, Phil. Mag. 19, 1207 (1969).
[11]C. Norris and H. P. Myers (unpublished); H. P. Myers, C. Norris, and B. Dellby (unpublished).
[12]D. H. Seib and W. E. Spicer, Phys. Rev. Letters 20, 1441 (1968); 22, 711 (1969); Phys. Rev. B 2, 1676 (1970); 2, 1694 (1970); L. Walldén, D. H. Seib, and W. E. Spicer, J. Appl. Phys. 40, 1281 (1969).
[13]W. B. Pearson, *A Handbook of Lattice Spacings and Structures of Metals and Alloys* (Pergamon, New York, 1958), Vol. 1.
[14]P. L. Hartman and E. Logothetis, Appl. Opt. 3, 255 (1964).
[15]P. O. Nilsson, Appl. Opt. 7, 435 (1968).
[16]W. E. Engeler, H. Fritzsche, M. Garfinkel, and J. J. Tiemann, Phys. Rev. Letters 14, 1069 (1965).
[17]M. Garfinkel, J. J. Tiemann, and W. E. Engeler, Phys. Rev. 148, 695 (1966); 155, 1046 (1967).
[18]E. M. Savitskii and N. L. Pravoverov, Zh. Neorgan. Khim. 6, 2776 (1961) [J. Inorg. Chem. 6, 1402 (1961)].
[19]E. M. Savitskii and N. L. Pravoverov, Zh. Neorgan. Khim. 6, 499 (1961) [J. Inorg. Chem. 6, 253 (1961)].
[20]R. H. Hubner, E. T. Arakawa, R. A. MacRae, and R. N. Hamm, J. Opt. Soc. Am. 54, 1434 (1964).
[21]H. Fröhlich and H. Pelzer, Proc. Phys. Soc. (London) A68, 525 (1955).
[22]H. Raether, Springer Tracts Mod. Phys. 38, 85 (1965).
[23]E. L. Green, Ph.D. thesis (Temple University, 1965) (unpublished); E. L. Green and L. Muldawer, Phys. Rev. B 2, 330 (1970).
[24]P. A. Wolff, Phys. Rev. 92, 18 (1953).
[25]H. Kanazawa, Progr. Theoret. Phys. (Kyoto) 13, 227 (1955).
[26]D. Pines, *Elementary Excitations in Solids* (Benjamin, New York, 1964).
[27]E. A. Taft and H. R. Phillip, Phys. Rev. 121, 1100 (1961).
[28]H. Ehrenreich and H. R. Phillip, Phys. Rev. 128, 1622 (1962).
[29]P. Dobberstein, A. Hampe, and G. Sauerbrey, Phys. Letters 27A, 256 (1968).
[30]S. N. Jasperson and S. E. Schnatterly, Phys. Rev. 188, 759 (1969).
[31]J. L. Stanford, H. E. Bennett, J. M. Bennett, E. J. Ashley, and E. T. Arakawa, Bull. Am. Phys. Soc. 13, 989 (1968).
[32]U. Gerhardt, Phys. Rev. 172, 651 (1968).
[33]B. R. Cooper, H. Ehrenreich, and H. R. Phillip, Phys. Rev. 138, A494 (1965).
[34]J. Daniels, Z. Physik 203, 235 (1967).

PHYSICAL REVIEW B VOLUME 3, NUMBER 12 15 JUNE 1971

Dielectric Theory of the Barrier Height at Metal-Semiconductor and Metal-Insulator Interfaces

K. Hirabayashi
Toshiba Research and Development Center,
Tokyo Shibaura Electric Company, Ltd., Kawasaki, Japan
(Received 21 December 1970)

The barrier height at metal-semiconductor and metal-insulator interfaces is calculated for a simple model of the system, in which the metal is replaced by a jellium model and the semiconductor and insulator by a continuum with a static dielectric constant. The spreading out of electronic charge into the dielectric continuum is determined by a variational procedure, which is an extension of the Smith's theory of the work function. Approximately, the calculated barrier height increases linearly with the work function of the metals. The slope increases with the ionicity of the semiconductors. The model, however, cannot explain the abrupt covalent-ionic transition.

The dependence of the barrier height ϕ_B at metal-semiconductor and metal-insulator interfaces on the work function ϕ_M of the metal is known to be approximated by the linear relation[1]

$$\phi_B = S\phi_M + \phi_0 , \tag{1}$$

where S and ϕ_0 are constants characteristic of the semiconductor and insulator. The slope S increases with ionicity from 0.1 (covalent materials) to 1 (ionic materials).

Recently it has been suggested by Phillips[2] that a theory of the barrier height may do without the knowledge of surface states. In this paper we consider the problem in the same spirit, but from a different point of view. We simplify the problem by introducing a model of the metal-semiconductor and metal-insulator systems, that is, a jellium model for the metal and a "dielectric continuum" model for the semiconductor and insulator. In the jellium model the positive charges are replaced by a uniform background of density

$$n_+(z) = n_+ , \quad z \leq 0 . \tag{2}$$